GSI-Preprint-97-36
Juli 1997

DECAY STUDIES OF THE NEUTRON-DEFICIENT ISOTOPES $^{114-118}$Ba

Z. Janas, A. Plochocki, J. Szerypo, R. Collatz, Z. Hu, H. Keller, R. Kirchner, O. Klepper, E. Roeckl, K. Schmidt, R. Bonetti, A. Guglielmetti, G. Poli, A. Piechaczek

(Submitted to Nucl. Phys. A)

Gesellschaft für Schwerionenforschung mbH
Planckstraße 1 • D-64291 Darmstadt • Germany
Postfach 11 05 52 • D-64220 Darmstadt • Germany

Decay studies of the neutron-deficient isotopes $^{114-118}$Ba

Z. Janas, A. Płochocki, J. Szerypo
Institute of Experimental Physics, Warsaw University, PL-00 681 Warsaw, Poland
R. Collatz, Z. Hu, H. Keller, R. Kirchner, O. Klepper, E. Roeckl, K. Schmidt
Gesellschaft für Schwerionenforschung, D-64220 Darmstadt, Germany
R. Bonetti, A. Guglielmetti, G. Poli
Istituto di Fisica Generale Applicata dell'Universitá di Milano, and Istituto Nazionale di Fisica Nucleare, Sezione di Milano, Milano, Italy
A. Piechaczek
Instituut voor Kern- en Stralingfysika, Katholieke Universiteit, B-3001 Leuven, Belgium

PACS: 23.40.-s; 23.20.Lv

Keywords: RADIOACTIVITY ^{114,115,116}Ba [from ^{58,60}Ni(^{58}Ni, xn), E=3.5-4.3 MeV/u]; ^{116,117,118}Ba [from ^{63}Cu(^{58}Ni, pxn), E=4.3-4.9 MeV/u]; Measured E_p, I_p, E_γ, I_γ, $\gamma\gamma$-coin, $T_{1/2}$; deduced cross-sections. Ge, Si, scintillator detectors, on-line mass separation

Abstract

The very neutron-deficient isotopes $^{114-118}$Ba were produced in ^{58}Ni induced reactions on ^{58}Ni, ^{60}Ni or ^{63}Cu targets. By on-line mass separation of BaF molecules formed in the separator ion source, exceptionally pure sources of these isotopes were available for spectroscopic studies. The β-decays of ^{114}Ba ($T_{1/2}=0.43^{+0.30}_{-0.15}$ s), ^{115}Ba ($T_{1/2}=0.45\pm0.05$ s), ^{116}Ba ($T_{1/2}=1.3\pm0.2$ s) and ^{118}Ba ($T_{1/2}=5.2\pm0.2$ s) were investigated for the first time. ^{114}Ba, ^{115}Ba and ^{116}Ba were identified as β-delayed proton emitters and absolute branching ratios for this decay mode were determined to be 20 ± 10 %, >15 %, and 3 ± 1 %, respectively. In the decay study of ^{118}Ba several γ transitions were identified. New information was also obtained on the β-delayed γ radiation of ^{117}Ba. The spectroscopic data were used to determine the production cross-sections for all these isotopes. Results of our half-life measurements and β-delayed proton studies are confronted with theoretical predictions.

1 Introduction

The decay studies of very neutron-deficient barium isotopes presented in this paper were motivated by theoretical calculations of Greiner et al. [1] and Poenaru et al. [2] who predicted the existence of a new island of cluster emitters in the vicinity of doubly magic ^{100}Sn, the most favorable case being ^{12}C emission from ^{114}Ba. It appeared interesting for us to look for the latter decay mode in a region of nuclei which are much lighter than those on the well established island of cluster radioactivity beyond ^{208}Pb. The results of this search experiment have been published elsewhere [3].

In this paper we present results of β-decay studies of $^{114-118}$Ba performed at the on-line mass-separator at GSI and aiming at half-lives measurements, identification of main decay modes, and determination of beam intensities for these isotopes. The importance of these studies stems, e.g., from the need of testing the ability of different theoretical calculations to predict β-decay rates of nuclei far from stability. Furthermore, the measured branching ratios ($b_{\beta p}$) and energy spectra of β-delayed protons (βp) allow one to verify the Q-values and the β-decay strength distributions applied in these calculations and may help to gain insight into the structure of studied nuclei. Additionally, from the measured intensities of mass-separated beams, information on the production cross-section of the investigated barium isotopes can be obtained and compared with the predictions of theoretical models.

One of the difficulties encountered in decay studies of nuclei very far from the valley of stability is the strong decrease in production rate for the most exotic nuclear systems. Moreover, due to the limited selectivity of the production reactions, the nuclei of interest are usually overwhelmed by other reaction products. In such cases separation techniques have to be used in order to select the desired species for spectroscopic studies. In β-decay studies at on-line mass separators with a chemically unselective ion source, mass separation suppresses most of the unwanted activity but leaves the problem of isobaric contaminants. Their decays increase the background activity to a level which often hinders the observation of the decay of interest, especially if β-delayed radiation of the investigated isotope has features similar to those of the contaminants.

In the case of β-decay studies of very neutron-deficient barium isotopes one faces all difficulties mentioned above. On the basis of statistical fusion-evaporation codes, one expects low reaction cross-sections (in the range of microbarns) for $^{114-118}$Ba as well as the presence of strong isobaric contamination by cesium isotopes (and their decay daughters) which dominate over the respective barium activity due to the much higher production cross-section and 100%-efficient ionization in the thermal ion source routinely applied in studies of alkaline earth isotopes. These difficulties are reflected in the experimental data available so far. Prior to our studies the lightest known barium

isotope was ^{117}Ba identified in the late seventies [4] by the observation of its β-delayed proton decay, while nothing was known about the decay of ^{118}Ba. Definitely, a new study of β-decay properties of very neutron-deficient barium isotopes required the development of a separator ion source with high chemical selectivity for barium. This aim was reached by applying the fluorination technique [5].

The following section describes the experimental techniques applied for the separation of barium isotopes and for radiation detection. Section 3 presents the results of the decay studies of $^{114-118}$Ba. The results of cross-section evaluations based on collected spectroscopic data are given in Section 4. In Section 5 the results of the half-life and βp measurements are discussed. Section 6 gives a summary and presents an outlook.

2 Experimental techniques

Neutron-deficient barium isotopes were produced in fusion-evaporation reactions between a 40 particle·nA ^{58}Ni beam from the linear accelerator UNILAC and a ^{58}Ni (2 mg/cm^2, enrichment 99.9%) or ^{60}Ni (2 mg/cm^2, enrichment 99.1%) target. The primary beam energy of 4.9 MeV/u was decreased to about 4.2 MeV/u on the nickel target by using a niobium or ^{63}Cu foil (2 mg/cm^2, enrichment 95.5%) as a degrader. In the latter case, the ^{63}Cu foil served also as a target for production of ^{116}Ba, ^{117}Ba, and ^{118}Ba.

The barium isotopes were prepared for spectroscopic studies by the GSI on-line mass-separator. Reaction products recoiling out of the target were stopped in a thin tantalum catcher inside the hot ion source of the separator, evaporated, ionized, accelerated to 55 keV and magnetically mass-separated. Up to three masses were investigated simultaneously in the three beam lines of the mass separator. Use of a thermoionizer of the cavity-type [6], operating at 2300-2400 K, removed all contaminants except cesium. Addition of CF_4 vapour into the thermoionizer converted barium very efficiently to BaF^+ ions, thus suppressing also cesium, which does not form fluoride ions, by at least 5 orders of magnitude. The properties of the fluorination ion source were investigated in separate, dedicated measurements and, in particular, the half-life dependence of the separation efficiency for the BaF^+ ions was determined [7].

For the study of the β-decay of ^{114}Ba and other neutron-deficient barium isotopes we used three different detection set-ups:

(A) The mass-separated beam was implanted into a tape in front of a β counter composed of a 0.7 mm thick, 24 mm diameter silicon detector followed by a 1 mm thick, 50 mm diameter plastic scintillator. Beta particles were registered with an efficiency of 25±3% by requiring coincidence between signals from the silicon and the scintillator detector. To avoid buildup of daughter activities, the tape periodically removed the

source from the detector. The observed grow-in of the collected activity was used to determine the decay half-life.

(B) The mass-separated beam was alternately stopped on a thin carbon foil in front of one of two ΔE–E telescopes. They consisted of 22 μm, 150 mm^2 and 700 μm, 450 mm^2 silicon surface-barrier detectors, respectively, and enabled background-free detection of protons or alpha particles with an efficiency of 17±1 %. By coincident summation of ΔE and E signals, energy spectra of β-delayed protons or alpha particles were obtained. The half-life of the collected activity was determined from the measured grow-in and decay pattern.

(C) The mass-separated beam was implanted in a second tape and periodically transported into the center of a U-shaped, 1 mm thick scintillator detector which was used to count β particles with an efficiency of 70±8 %. X-rays and low energy γ-rays were recorded by using a 2000 mm^2 planar germanium detector, whereas higher-energy γ radiation was registered by a germanium detector with a standard efficiency of 15 %. The two germanium detectors were placed on opposite sides of the tape at a distance of about 7 mm from it.

Coincidence signals from the detectors were recorded in event by event mode. To determine the half-lives of the studied activities, the time of occurrence of each event was stored together with energy and fast timing information. The energy signals of the β- and γ-rays detectors were also collected as singles in multispectra mode.

3 Results

3.1 Decay of ^{114}Ba

The knowledge of the half-life and the intensity of the $^{114}BaF^+$ beam were necessary to set a lower limit for the partial half-life of ^{12}C emission from this isotope [3]. Both these quantities were determined by detecting positrons emitted in the β-decay of ^{114}Ba. In these measurements the mass-separated beam of $^{114}BaF^+$ ions was implanted into the collection tape in front of the β-telescope (detection set-up A) and the grow-in of the activity was observed. Every 2 seconds the tape transport system moved the source away and initiated a new collection cycle.

Fig. 1 shows the time distribution of positrons registered simultaneously in both detectors of the β-telescope within 24 hours of measurements. The resulting grow-in distribution inevitably contains components from the decay products of ^{114}Ba. However, since ^{114}Ba was the only radioactive isotope present in the mass-separated beam, the experimental positron grow-in curve can be described by a function which contains as free

parameters a constant background level, the $^{114}BaF^+$ beam intensity, half-life of ^{114}Ba and its probability of βp emission. The contribution of the ^{114}Ba daughter activities can be calculated since the decay modes and the half-lives of all ^{114}Ba descendants in the A=114 chain, including the decay properties of the A=113 isobars populated in the βp decay of ^{114}Ba and ^{114}Cs, are known. The least-square fitting procedure (see Fig. 1) yielded $T_{1/2}=0.43^{+0.30}_{-0.15}$ s for the ^{114}Ba half-life and an intensity of 0.12±0.04 $^{114}BaF^+$ ions/s, normalized to a ^{58}Ni beam current of 40 particle·nA.

We found, however, that the fit results for the half-life and for the separation rate weakly depend on the $b_{\beta p}$ value of ^{114}Ba. Therefore, the latter quantity was determined in an additional measurement by using detection set-up B. The beam was switched between the telescopes every 3 s. Fig. 2 shows the energy spectrum of βp measured during 60 hours of ^{114}BaF source collection. No events corresponding to β-delayed alpha particles were detected in this measurement. Not all registered proton events originate from the decay of ^{114}Ba: ^{114}Cs emits protons with a probability of 7±2 % [8], whereas a limit of 1.4 - 12.4 % has been found for the $b_{\beta p}$ value of ^{113}Xe [9]. Since all ^{114}Cs and ^{113}Xe atoms were produced through the decay of ^{114}Ba, one can express the measured proton counting rate by the implantation rate of $^{114}BaF^+$ ions and the $b_{\beta p}$ values of the three contributing proton emitters. The only unknown quantity in this expression, i.e. the probability of βp emission for ^{114}Ba, was determined as 20±10 %, assuming that the ^{114}Ba separation rate equals that observed in the positron measurements. This assumption is justified since (i) the observed proton rate was stable during the whole measurement, (ii) the same proton rate was observed before and after positron counting.

The consistency of the experimental half-life and $b_{\beta p}$ value for ^{114}Ba was confirmed in the analysis of the proton grow-in and decay pattern. Good agreement between the calculated and experimental time distribution was obtained.

3.2 Beta decay of ^{115}Ba

One expects that the energy window of almost 11 MeV [10] for βp emission from ^{115}Ba leads to a high probability of this decay mode. Therefore, in our searches for the unknown ^{115}Ba we concentrated on proton detection. Set-up B was used to measure the energy and time characteristics of β-delayed particles emitted from the mass-separated sources. During 115 hours of data collection with the ^{58}Ni target, a total number of 1680 protons was registered; a much higher rate was achieved in measurements with the ^{60}Ni target, where 300 protons were observed within 3.5 hours. No events corresponding to β-delayed alpha particles were observed in these measurements. The ΔE+E energy spectrum of all registered protons is shown in Fig. 2, whereas Fig. 3 shows the time distribution of protons observed in measurements with the ^{115}BaF beam being switched between the

telescopes every 4 seconds.

The registered proton spectra contain a contribution from two products of the ^{115}Ba decay, i.e. ^{115}Cs ($T_{1/2}$=1.4±0.8 s) and ^{115}Xe ($T_{1/2}$=18±4 s) with $b_{\beta p}$ values of about $7 \cdot 10^{-4}$ [11] and $(3.4 \pm 0.6) \cdot 10^{-3}$ [11], respectively. From the observed time characteristics one can judge, however, that most of the protons originate from a short-lived activity since the dominance of a long lived one, e.g. ^{115}Xe, would result in a flat time distribution. This unknown short-lived proton activity we assigned to the βp decay of ^{115}Ba.

The half-life and the $b_{\beta p}$ value of ^{115}Ba were determined by fitting the theoretical time distribution that included all βp components in A=115 chain, to the measured time spectrum. Since the half-lives and the $b_{\beta p}$ values of ^{115}Cs and ^{115}Xe are known, the theoretical time distribution was parametrized only by the ^{115}Ba half-life and its $b_{\beta p}$ value. The least-square fit yielded $T_{1/2}$=0.45±0.05 s for the decay half-life of ^{115}Ba and a lower limit of 15% for $b_{\beta p}$.

3.3 Beta decay of ^{116}Ba

The measurements of ^{116}Ba were based on the detection of β-delayed X-rays and protons in set-up C and B, respectively. In the former measurement, the activity was produced using a ^{60}Ni target and transported in front of the detectors in a 4 s cycle. Fig. 4 shows the β-gated energy spectrum of X-rays registered during 5 hours of data collection. The requirement of a coincidence with positrons prevents the detection of cesium X-rays originating from the presumably dominant electron conversion of a possible transition connecting the 0.7 s and 3.8 s metastable states known in ^{116}Cs [12]. Therefore, the pronounced peaks of the Cs KX-rays occurring in the spectrum shown in Fig. 4 constitute a firm signature of the observation of ^{116}Ba decay. The time characteristics of the Cs KX-rays intensity (see inset in Fig. 4), analyzed under the assumption of a single decay component, yielded $T_{1/2}$=1.3±0.2 s for the half-life of ^{116}Ba.

The Xe KX-rays peak visible in Fig. 4 as well as a 394 keV line seen in the γ-rays spectrum originate from the β-decay of ^{116}Cs which is produced by ^{116}Ba decay. The time dependance of the intensity of the Xe KX-rays follows the distribution expected for the decay of ^{116}Cs from the 0.7 s state. Since the same time behaviour was observed for the intensity of the 394 keV line, and since no trace of γ-rays characteristic for the decay of 3.8 s ^{116}Cs state was found, we conclude that the β-decay of ^{116}Ba selectively populates ^{116}Cs in the 0.7 s state.

To search for β-delayed particle emission from ^{116}Ba the mass-separated $^{116}BaF^{+}$ beam was switched between two ΔE-E telescopes (detection set-up B) every 6 s. During 5 hours of measurement with the ^{63}Cu target and 6 hours of measurement with the ^{60}Ni target, we registered 35 and 150 protons (see Fig. 2), respectively. No events

corresponding to β-delayed alpha particles were observed. The half-life of the proton activity, estimated by comparing the number of counts observed during collection and decay periods for each telescope, was found to be close to the ^{116}Ba half-life of 1.3±0.2 s (see above). This observation indicates that ^{116}Ba is the main source of the A=116 proton activity. A contribution to the measured proton spectra is expected from two decay products of the ^{116}Ba, i.e. ^{116}Cs (0.7 s) and ^{115}Xe. The latter two isotopes have $b_{\beta p}$ values of $(2.8\pm0.7)\cdot10^{-3}$ [12] and $(3.4\pm0.6)\cdot10^{-3}$ [11], respectively.

The $b_{\beta p}$ value of ^{116}Ba was determined by relating the $^{116}BaF^+$ beam intensity to the observed proton rate, correcting the latter for contribution from the ^{116}Cs and ^{115}Xe decays. To avoid a systematic uncertainty due to the long-term instability of the separator ion source, both rates were determined in measurements that followed each other immediately.

The $^{116}BaF^+$ beam intensity was measured by counting positrons emitted from samples collected during 6 s cycles in front of the β-telescope (detection set-up A). The measured grow-in curve was fitted to the time distribution expected for positrons emitted from the decays of ^{116}Ba, ^{116}Cs (0.7 s), ^{116}Xe, and ^{116}I, the only free parameters being a constant background level and the separation rate of ^{116}Ba. For the ^{60}Ni target the $^{116}BaF^+$ beam intensity was determined to be 0.04±0.01 molecules/s normalized to 1 particle·nA ^{58}Ni beam current, whereas the corresponding βp rate amounted to $(1.5\pm0.3)\cdot10^{-3}$ protons/s. From these values one obtains 3±1 % for the $b_{\beta p}$ value of ^{116}Ba.

3.4 The nuclide ^{117}Ba

The decay of ^{117}Ba was identified for the first time by Bogdanov et al. [4, 13], who observed the βp emission from this isotope, measured its half-life, and determined the energy window for βp decay. The analysis of the βp energy spectrum based on statistical model calculations indicated the existence of a resonance in the β-strength distribution of ^{117}Ba [13, 14]. The possible presence of a structure in the β-strength function of ^{117}Ba was further investigated by studying βp-γ-ray coincidences [15]. Proton transitions leading to the ground state and two excited states in ^{116}Xe were observed and the relative branching ratios were determined.

Fig. 2 shows the energy spectrum of βp from ^{117}Ba collected in this work by using detection set-up B. The measured spectral shape of β-delayed protons is compatible with the one determined in earlier studies [4, 13].

Below we report on the first observation of β-delayed γ-rays of ^{117}Ba. The decay of ^{117}Ba was studied by using detection set-up C with the tape transporting the collected activity every 4 s. Fig. 5 shows the energy spectrum of X-rays and low-energy γ-

rays registered in coincidence with positrons during 12 hours of measurement. The decay curve of the β-gated Cs KX-rays yielded a value of 1.6±0.2 s for the half-life of ^{117}Ba (see Fig. 6), in agreement with the values obtained in βp studies of this nucleus [4, 13, 15]. Gamma lines, whose half-lives are compatible with 1.6±0.2 s (see Fig. 6), were ascribed to the decay of this isotope. Moreover, since none of these lines were seen in coincidence with the ^{117}Ba β-delayed protons [15], we assign them to the decay of excited states in ^{117}Cs fed in the β-decay of ^{117}Ba. Table 1 shows the energies, relative intensities and coincidence relationships for these γ-rays. Together with the information on transitions in ^{117}Cs, the relative intensity of the 364 keV $2^+ \rightarrow 0^+$ transition in ^{116}Xe is given. This line appears in the γ-rays spectrum due to the βp branch in the decay of ^{117}Ba, as reported in [15]. We observed also several known γ lines from the decay of ^{117}Cs, the strongest one being the 205 keV doublet emitted with a probability of 218±16 transitions per 1000 ^{117}Cs decays [16]. Due to the chemical selectivity of the fluorination ion source, all ^{117}Cs nuclei decaying in front of the detectors originate exclusively from the disintegration of ^{117}Ba. Therefore, by measuring the intensity of the 205 keV line, and by taking into account the cycle time of the tape transport system as well as the half-lives of ^{117}Ba and ^{117}Cs, we determined the number of collected ^{117}Ba atoms which were transformed into ^{117}Cs. Similarly, from the intensity of the 364 keV $2^+ \rightarrow 0^+$ transition in ^{116}Xe we found the number of collected ^{117}Ba atoms which decayed with βp emission. By combining these two numbers it was possible to determine the $b_{\beta p}$ value of ^{117}Ba to be 13±3% and to deduce the absolute intensities of the γ transitions per ^{117}Ba decay; a factor of 0.053±0.010 % should be used to obtain the latter intensities from the relative values given in Table 1.

3.5 Beta decay of ^{118}Ba

Nothing was known about the decay of ^{118}Ba prior to our studies. The rather small energy window for βp emission from this isotope (4.7±0.5 MeV [10]) is expected to yield a small $b_{\beta p}$ value. Therefore, we used the detection set-up C to identify the decay of ^{118}Ba and to search for the β-delayed gamma radiation from this isotope.

Fig. 7 shows the energy spectrum of low energy γ-rays registered in coincidence with positrons during 12 hours of measurement with a 12 s collection cycle. The decay of ^{118}Ba was unambiguously identified by the observation of cesium X-rays in this spectrum. From the time characteristics of the Cs KX-rays intensity the ^{118}Ba half-life of $T_{1/2}$=5.2±0.2 s was determined under the assumption of a single decay component. As shown in Fig. 8, similar half-lives were found for several of the observed γ-lines.

Table 2 lists the energies, intensities and coincidence relationships of the γ-lines assigned to the decay of ^{118}Ba. The final assignment was based on the results of the half-life

analysis and/or on the observed coincidence relations. In order to determine the absolute branching ratios for the γ transitions given in Table 2, we used again the advantage that all contaminants of the initially clean ^{118}Ba source are β-decay descendants of this nucleus. The most prominent contamination line visible in the γ-ray spectrum was the 337 keV $2^+ \rightarrow 0^+$ transition in ^{118}Xe [17]. We assigned this transition to the decay of the low spin (probably I=2), $T_{1/2}$=14±2 s ^{118}Cs state [17]. A contribution from the β-decay of the high spin (I=6, 7, 8) $T_{1/2}$=17±3 s isomer in ^{118}Cs [17] was excluded since we did not observe the 587 keV transition deexciting the 1366 keV 6^+ level in ^{118}Xe, known to be strongly populated in the β-decay of 17 s ^{118}Cs [17]. From the existing decay scheme of ^{118}Cs [17] we deduced that 86±5 % of the decays of the low spin state in ^{118}Cs lead to the emission of the 337 keV line. This branching ratio, the measured intensity of the 337 keV line, the known decay half-lives of ^{118}Ba and ^{118}Cs, and the length of the tape transport cycle permit the determination of the number of ^{118}Ba atoms which decayed in front of the detectors. The straightforward calculation yields a conversion factor of 0.20±0.04 % which should be used to convert the relative intensities given in Table 2 into the absolute γ-ray emission probabilities.

4 Cross-sections evaluations

As described in the preceding section, our spectroscopic studies of neutron-deficient barium isotopes allowed us to determine half-lives as well as absolute branching ratios for the observed decay modes of $^{114-118}$Ba. Therefore, since the efficiencies of our detection set-ups were measured with standard calibration procedures, it was possible to deduce the BaF^+ intensities for these isotopes. By correcting the latter value for the known (and half-life dependent) separation efficiency for BaF^+ ions [7] and the 80% transmission through the separator one obtains the production rate of a given isotope in the target. It was assumed that all (barium) reaction products recoil without any intensity loss into the catcher mounted in the ion source. Finally, since the ^{58}Ni beam dose during the target irradiation was measured, one can determine production cross-sections averaged across the target thickness.

Table 3 summarizes the relevant data. The reactions are specified in the first column. In the second column, the ranges of projectile energies in the target are given. The third column of Table 3 lists the BaF^+ beam intensities. The last column gives the cross-sections determined in this work.

The comparison of the experimental production cross-sections with values predicted by the HIVAP code [18] reveals the tendency of this code to overestimate the production cross-section for isotopes far from stability. A similar conclusion has already been drawn

for the case of tin isotopes [19, 20, 21].

5 Discussion

In Table 4, the results of our new experimental half-lives and $b_{\beta p}$ values are collected and compared with the results of two theoretical calculations which represent different approaches in the description of the β-decay strength function. The gross theory [22] is based on sum rules of the β-decay strength function and treats the transitions to all final states in a statistical manner. In the microscopic calculations of Hirsch et al. [23] matrix elements of the Gamow-Teller (GT) transitions, which dominate in the β-decay of studied nuclei, are calculated in the proton-neutron quasiparticle random-phase approximation (pn-QRPA). Both, the particle-hole (ph) and particle-particle (pp) like channels of the residual proton-neutron interaction, were included in the definition of the QRPA matrix equation. A similar approach is presented in the recent nuclear-structure calculations of Möller et al. [24]. Although in this case the particle-particle correlations were neglected in the QRPA treatment, the β-strength functions calculated for $^{114-118}$Ba resemble very much those derived by Hirsch et al. [23] and will not be further discussed in this paper.

Fig. 9 shows the β-strength distribution for $^{114-117}$Ba predicted by the gross theory and pn-QRPA calculations of Hirsch et al.. The very smooth energy dependence of the β-strength function predicted by the gross theory reflects the statistical nature of this model while the much more complex shape of the GT strength distribution obtained in the pn-QRPA calculations is thought to reflect the underlying intrinsic nuclear structure.

It is evident that both calculations do not only give quite different shapes of the β-strength distribution, but also deviate significantly in the predictions of the total strength within the Q_{EC} window. In spite of this, the half-life estimates based on the gross theory as well as on the pn-QRPA calculations agree with each other and very well reproduce the measured values. This result clearly indicates that the verification of β-strength calculations based only on the examination of predicted half-lives is not conclusive.

However, another attempt to test the theoretical β-strength distribution can be made, if one uses these strength functions to reproduce the energy spectra of β-delayed protons observed in the decays of the studied nuclei. Therefore, we performed statistical model calculations [25, 26] of β-delayed proton spectra from $^{114-118}$Ba, consistently applying the same Q-values and β-strength functions which were used to predict half-lives.

The probability of proton emission leading to the ground state and to the known excited states in the final nucleus was calculated using the set of optical model parameters from ref. [27] and the back-shifted Fermi-gas level density formula [28] with parameters

recommended by Hardy [29]. For ^{114}Ba and ^{116}Ba only transitions to the ground state of the final nucleus were considered due to the lack of experimental information on the excited states in the ^{113}Xe and ^{115}Xe. The resulting βp branching ratios are given in Table 4 as a range of values obtained when the Q_{EC} and S_p energy is arbitrarily changed by $\pm$250keV relative to the value given by the mass formulas used to predict half-lives.

A comparison of experimental and calculated $b_{\beta p}$ data indicates that values obtained with the use of the β-strength function from the pn-QRPA calculations agree, within the error bars, with the measured ones, while the βp branches calculated with the gross theory β-strength distribution are systematically underestimated. In the case of the ^{116}Ba decay, even if one accounts for the Q-values uncertainties, the $b_{\beta p}$ value obtained with the gross theory β-strength function is an order of magnitude lower than the experimental result.

Fig. 2 illustrates the influence of the applied β-strength function on the shape of the calculated proton spectra. The essentially structureless β-strength function predicted by the gross theory reasonably well reproduces the shape of measured βp energy spectra for ^{114,116,117}Ba. For ^{115}Ba, however, the proton energy spectrum calculated by using the gross theory β-strength function diverges significantly from the experimental one. For this isotope much better agreement between the shape of experimental and calculated proton spectra is obtained, when the β-strength distribution predicted by the pn-QRPA calculations is used. Also for ^{116}Ba and ^{117}Ba the shape of βp energy spectra calculated with the pn-QRPA β-strength resembles the measured one, but a closer inspection indicates a deficiency of the model in the description of the splitting and fine structure of the β-strength distribution in the decays of these isotopes. In the case of ^{114}Ba the βp energy spectrum calculated with the use of pn-QRPA strength function is shifted with respect to the measured one by about 2 MeV towards higher energies. This discrepancy cannot be removed even if one considers possible transitions to (so far experimentally unknown) excited states in the ^{113}Xe or accounts for ambiguities in the predicted Q_{EC} and S_p values. Evidently the pn-QRPA calculations place the broad resonance structure visible in the β-strength distribution for ^{114}Ba decay at too high excitation energies in the daughter nucleus. In the pn-QRPA calculations the position of this resonance depends mainly on the strength of the ph force of the GT interaction, whereas the inclusion of the pp force and the deformation leads to the suppression and redistribution of the calculated β-strength. In the approach presented in ref. [23] the strengths of pp and ph interactions were held fixed within an isotopic chain and adjusted to reproduce the known half-lives. Since the dependence of the calculated half-lives on the strength of the ph interaction is reduced with increasing distance from stability, such a procedure turns out to be successful in prediction of the half-lives of unknown isotopes. However,

as discussed in ref. [23], the values obtained for the strength of ph interaction are rather uncertain and may vary from one isotope to another. This may explain why the reasonable agreement between the calculated and measured proton spectra obtained for ^{115,116,117}Ba does not hold for ^{114}Ba.

From the results of our studies of βp decay we conclude that the β-strength function from the pn-QRPA calculations provides a reasonable description of the shape and intensity of the βp energy spectra for ^{115,116,117}Ba but it fails to reproduce the βp spectrum for ^{114}Ba. The origin of this disagreement cannot be firmly identified without systematic studies of the β-strength distribution at high excitation energies. In view of the serious disagreement between the measured and calculated $b_{\beta p}$ values, the ability of reproducing the βp energy spectrum shape by using the gross theory strength function seems to be accidental and cannot be considered as a proof that this theory provides a reasonable approximation of the β-strength function in the decays of the studied nuclei. The situation is well illustrated in the case of ^{116}Ba and ^{117}Ba, where the maximum intensity of the proton spectrum calculated by using the gross theory strength function appears almost at the same energy as the maximum corresponding to the resonance visible in the pn-QRPA strength distribution at about 4.5 MeV excitation energy. Obviously, accounting for these local resonances increases the $b_{\beta p}$ values and gives good agreement with experiment.

6 Summary and outlook

In summary, by application of a chemically selective ion source at the GSI on-line mass separator four new barium isotopes were identified and their main decay properties were studied for the first time. The half-lives, energy spectra and branching ratios of β-delayed protons as well as production cross-sections determined in this work were confronted with model predictions. In spite of good agreement between the experimental and calculated decay rates, the analysis of the βp energy spectra indicates deficiencies in the theoretical description of the β-decay strength function. The production cross-sections measured for barium isotopes cannot be reproduced by the HIVAP code. Clearly, a more complete set of experimental data is needed for a quantitative analysis and improvement of cross-sections calculations.

The experiments described in this work, which have yielded gross properties for very neutron-deficient barium isotopes could be extended in several ways. Improved high-resolution γ-ray coincidence and conversion electron measurements would allow one to establish partial decay schemes of ^{116}Ba, ^{117}Ba and ^{118}Ba at least for low excitation energies of the respective daughter nuclei. These measurements can be complemented

by the application of a total absorption spectrometer [31] for β-decay strength function determination. Further studies of βp emission, e.g. βp-γ coincidence measurements, should remove ambiguities of parameters used in theoretical description of the process. New γ-ray and βp measurements, together with the indispensable (and so far unavailable) experimental information on the decay Q-values, may lead to a more demanding test of theoretical β-strength calculations.

7 Acknowledgements

We would like to thank K. Burkard and W. Hüller for their competent technical support and B. Paulik and T. Pytlik for their contribution made within the framework of the GSI International Student Program 1994. We are indebted to M. Hirsch, B. Pfeiffer and T. Tachibana for providing us with the results of their β-strength calculations. This work was supported in part by the European Community under Contracts No. ERBCIPD-CT-940091 and ERBCIPD-CT-950083. The authors from Warsaw would like to acknowledge support and hospitality of GSI and partial support from the Polish Committee of Scientific Research under grant KBN 2 P03B 039 13. One of us (Z. J.) would like to acknowledge support from the Alexander von Humboldt Foundation. The analysis of the data presented in this paper was performed using a workstation donated by this Foundation to the University of Warsaw.

References

[1] W. Greiner, M. Ivascu, D.N. Poenaru, and A. Sandulescu, in *Treatise on Heavy Ion Science*, edited by D.A. Bromley (Plenum, New York,1989), Vol. 8, p. 641

[2] D.N. Poenaru, D. Schnabel, W. Greiner, D. Mazilu, R. Ghergescu, At. Data Nucl. Data Tables **48** (1991) 231

[3] A. Guglielmetti, R. Bonetti, G. Poli, P.B. Price, A.J. Westphal, Z. Janas, H. Keller, R. Kirchner, O. Klepper, A. Piechaczek, E. Roeckl, K. Schmidt, A. Płochocki, J. Szerypo and B. Blank, Phys. Rev. **C52** (1995) 740

[4] D.D. Bogdanov, A.V. Demyanov, V.A. Karnaukhov, L.A. Petrov, A. Płochocki, V.G. Subbotin and J. Voboril, Nucl. Phys. **A275** (1977) 229

[5] R. Eder, H. Grawe, E. Hagebø, P. Hoff, E. Kugler, H.L. Ravn and K. Steffensen, Nucl. Instr. and Meth. in Phys. Res. **B62** (1992) 535

[6] R. Kirchner, Nucl. Instr. and Meth. in Phys. Res. **A292** (1990) 203

[7] R. Kirchner, GSI Scientijfic Report 94-1 (1995) 287, and Nucl. Instr. and Meth. in Phys. Res. **B**, in press

[8] E. Roeckl, G.M. Gowdy, R. Kirchner, O. Klepper, A. Piotrowski, A. Płochocki, W. Reisdorf, P. Tidemand-Petersson, J. Żylicz, D. Schardt, G. Nyman and W. Lindenzweig, Z. Phys. **A294** (1980) 221

[9] P. Tidemand-Petersson, R. Kirchner, O. Klepper, E. Roeckl, D. Schardt, A. Płochocki and J. Żylicz, Nucl. Phys. **A437** (1985) 342

[10] G. Audi and A.H. Wapstra, Nucl. Phys. **A565** (1993) 1

[11] J. Blachot and G. Marguier, Nucl. Data Sheets, **52** (1987) 565

[12] J. Blachot and G. Marguier, Nucl. Data Sheets, **73** (1994) 81

[13] D.D. Bogdanov, A.V. Demyanov, V.A. Karnaukhov, L.A. Petrov, J. Voboril, Nucl. Phys. **A303** (1978) 145

[14] P. Tidemand-Petersson and A. Płochocki, Phys. Lett **118B** (1982) 278

[15] P. Tidemand-Petersson, R. Kirchner, O. Klepper, E. Roeckl, D. Schardt, A. Płochocki, J. Żylicz, Nucl. Phys. **A437** (1985) 342

[16] J. Blachot, and G. Marguier, Nucl. Data Sheets **50** (1987) 63

[17] K. Kitao, Nucl. Data Sheets **75** (1995) 187

[18] W. Reisdorf, Z. Phys. **A300** (1981) 227; GSI-Rep. **81-2** (1981) 73

[19] R. Kirchner, O. Klepper, D. Marx, G.-E. Rathke and B. Scherrill, Nucl. Instr. and Meth. in Phys. Res. **A247** (1986) 265

[20] R. Barden, R. Kirchner, O. Klepper, E. Roeckl, A. Płochocki, G.-E. Rathke, K. Rykaczewski, D. Schardt, J. Żylicz, Z. Phys. **A329** (1988) 319

[21] Z. Janas, H. Keller, R. Kirchner, O. Klepper, A. Piechaczek, E. Roeckl, K. Schmidt, M. Huyse, J. von Schwarzenberg, P. Van Duppen, L. Vermeeren, F. Albus, H.-J. Kluge, G. Passler, F.P. Scheerer, N. Trautmann, V.N. Fedoseyev, V.I. Mishin, R. Grzywacz, A. Płochocki, K. Rykaczewski, J. Żylicz, Phys. Scripta **T56** (1995) 262

[22] K. Takahashi, Prog. Theor. Phys. **47** (1972) 1500; T. Tachibana, M. Yamada and Y. Yoshida, Prog. Theor. Phys. **84** (1990) 641

[23] M. Hirsch, A. Staudt, K. Muto, H.V. Klapdor-Kleingrothaus, Atomic Data Nucl. Data Tables **53** (1993) 165

[24] P. Möller, J.R. Nix, K.-L. Kratz, At. Data Nucl. Data Tables, in press

[25] P. Hornshøj, K. Wilsky, P.G. Hansen, B. Jonson, O.B. Nielsen, Nucl. Phys. **A187** (1972) 609

[26] B. Jonson, E. Hagberg, P.G. Hansen, P. Hornshøj, P. Tidemand-Petersson, Proc. 3rd Intern. Conf. on Nuclei far from Stability, Cargès (1976), CERN 76-13, p. 277

[27] C.M. Perey, and F.G. Perey, At. Data Nucl. Data Tables **17** (1976) 1

[28] W. Dilg, W. Schantl, H. Vonach, M. Uhl, Nucl. Phys. **A217** (1973) 269

[29] J.C. Hardy, Phys. Lett. **109B** (1982) 242

[30] P. Möller, J.R. Nix, W.D. Myers, W.J. Swiatecki, At. Data Nucl. Data Tables **59** (1995) 185

[31] M. Karny, J.M. Nitschke, L.F. Archambault K. Burkard, D. Cano-Ott, M. Hellstöm, W. Hüller, R. Kirchner, S. Lewandowski, E. Roeckl, A. Sulik, Nucl. Instr. and Meth. in Phys. Res. **B**, in press

[32] T. Tachibana, M. Uno, M. Yamada, S. Yamada, At. Data Nucl. Data Tables **39** (1988) 251

[33] P. Möller and J.R. Nix, At. Data Nucl. Data Tables **26** (1981) 165

Table 1: Energies, relative intensities and coincidence relations for the γ-rays observed in the decay of ^{117}Ba.

E_γ(keV)	I_γ^{rel}[a]	Coincident γ-lines
45.7(1)	12(2)[b]	511
78.0(1)	12(2)[b]	511
87.5(1)	34(3)[b,c]	CsKX, 94.9, 511
94.9(1)	100(7)	CsKX, 87.5, 511
101.6(1)	70(6)	CsKX, 511
363.6(2)[d]	113(18)[e]	511

[a] Absolute intensities per 100 decays are obtained by multiplying I_γ^{rel} by 0.053±0.010

[b] Gamma-ray intensity deduced from the β-gated spectrum

[c] Intensity corrected for the contribution from the fluorescence Pb $K_{\beta 2}$X-rays

[d] $2^+ \rightarrow 0^+$ transition in ^{116}Xe following the βp decay of ^{117}Ba

[e] Intensity corrected for the contribution from the ^{117}Cs decay

Table 2: Energies, relative intensities and coincidence relations for the γ-rays observed in the decay of ^{118}Ba.

E_γ(keV)	I_γ^{rel}[a]	Coincident γ-lines
40.1(1)	15(2)	511
52.3(1)	100(5)	CsKX, 126.3, 156.2, 511
61.7(1)	30(2)	511
64.9(1)	69(4)	511
76.1(1)	31(2)	CsKX, 511
79.3(1)	19(2)	CsKX, 511
92.5(1)	45(3)	511
126.3(2)	16(2)[b]	511
129.3(2)	24(2)[b]	79.3, 511
156.2(2)	33(3)	CsKX, 52.3, 511

[a] Absolute intensities per 100 decays are obtained by multiplying I_γ^{rel} by 0.20(4)

[b] Gamma-ray intensity deduced from the β-gated spectrum

Table 3: BaF^+ beam intensities and production cross-sections for neutron-deficient barium isotopes.

Reaction	Energy (MeV/u)	Intensity $(\frac{BaF^+/s}{1particle \cdot nA})$	σ_{exp} (μb)
^{58}Ni(^{58}Ni, 2n)^{114}Ba	3.5 - 4.2	$3(1)\cdot10^{-3}$	$0.20^{+0.13}_{-0.09}$
^{58}Ni(^{58}Ni, 1n)^{115}Ba	3.5 - 4.2	$< 3\cdot10^{-3}$	< 0.2
^{60}Ni(^{58}Ni, 3n)^{115}Ba	3.6 - 4.3	$< 2\cdot10^{-2}$	< 1
^{58}Ni(^{58}Ni, 0n)^{116}Ba	3.5 - 4.3	$< 3\cdot10^{-4}$	< 0.03
^{60}Ni(^{58}Ni, 2n)^{116}Ba	3.6 - 4.3	$4(1)\cdot10^{-2}$	3(1)
^{63}Cu(^{58}Ni, 1p4n)^{116}Ba	4.3 - 4.9	$8(3)\cdot10^{-3}$	0.8(4)
^{63}Cu(^{58}Ni, 1p3n)^{117}Ba	4.3 - 4.9	$6(2)\cdot10^{-1}$	55(20)
^{63}Cu(^{58}Ni, 1p2n)^{118}Ba	4.3 - 4.9	$4(1)\cdot10^{-1}$	19(6)

Table 4: Comparison of half-lives and $b_{\beta p}$ values, measured for neutron-deficient barium isotopes, with theoretical predictions. The Q_{EC} values listed are those of the parent (barium) isotopes, while the S_p values are given for the daughter (cesium) isotopes.

			Q_{EC}[a]	$S_\beta^{Gross-Th.}$		Q_{EC}[b]	S_β^{QRPA}	
Isotope I^π	$T_{1/2}^{exp}$ (s)	$b_{\beta p}^{exp}$ (%)	S_p (MeV)	$T_{1/2}$ (s)	$b_{\beta p}$ (%)	S_p (MeV)	$T_{1/2}$ (s)	$b_{\beta p}$ (%)
^{114}Ba	$0.43(^{+30}_{-15})$	20(10)	8.91	0.3	2-7	9.83	0.3	15-26
0^+			-0.15			0.01		
^{115}Ba	0.45(5)	>15	10.63	0.4	19-46	10.98	0.4	20-37
$(3/2^-)$			-0.10			0.24		
^{116}Ba	1.3(2)	3(1)	7.90	0.9	0.03-0.17	8.03	1.0	0.5-3
0^+			0.92			0.82		
^{117}Ba	1.6(2)	13(3)	9.17	1.9	3-10	9.26	2.4	9-23
$3/2^+$			0.70			1.0		
^{118}Ba	5.2(2)	-	6.22	5.5	0.01-0.06	6.56	9.5	0.03-0.4
0^+			1.40			1.57		

[a] Q_{EC} and S_p values from ref. [32]

[b] Q_{EC} and S_p values from ref. [33]

Figure 1: Time distribution of positrons registered in the β-telescope during 24 hours of ^{114}BaF beam collection. The solid line shows the result of a least-square fit of the theoretical curve to the experimental data points. The dashed line displays the contribution from room background and from decay of the ^{114}Ba descendants ^{114}Cs, ^{114}Xe, ^{114}I as well as ^{113}Xe, ^{113}I and ^{113}Te.

Figure 2: Energy spectra of β-delayed protons (full circles) registered during collection of beams of ^{114}BaF (60 hours), ^{115}BaF (115 hours), ^{116}BaF (11 hours) and ^{117}BaF (5.5 hours), respectively. The experimental ^{114,115,116}Ba spectra contain contributions of 25%, $< 3\%$ and 9%, respectively, of βp from barium decay products (see Section 3 for details). The solid-line histograms represent the βp energy spectra calculated by using the β-strength from the pn-QRPA calculations, whereas the dashed-line histograms show the results obtained by using β-strength distribution from the gross theory. The theoretical and experimental spectra were normalized to equal integral number of counts.

Figure 3: Grow-in and decay spectrum of β-delayed protons registered during ^{115}BaF measurements. The solid line represents the best fit of the theoretical multi-component time distribution to the experimental data.

Figure 4: Energy spectrum of X-rays registered in coincidence with positrons during 5 hours of ^{116}BaF measurement. The inset shows the time characteristics of Cs KX-rays intensity. The solid line represents the best fit of the one-component decay curve to the experimental data.

Figure 5: Energy spectrum of X-rays and low energy γ-rays registered in coincidence with positrons during 12 hours of ^{117}BaF beam collection. γ-lines labeled by their energies were identified as transitions in ^{117}Cs that follow β-decay of ^{117}Ba.

Figure 6: Time characteristics of the intensities of the β-gated Cs KX-rays and 46, 87, 95 and 102 keV γ-lines ascribed to the decay of ^{117}Ba. The solid lines represent the best fits of the one-component decay curves to the experimental data.

Figure 7: Energy spectrum of X-rays and low energy γ-rays registered in coincidence with positrons during 12 hours of ^{118}BaF beam collection. γ-lines labeled by their energies were attributed to the decay of ^{118}Ba.

Figure 8: Time distribution of the intensities of β-gated Cs KX-rays and 40, 52, 65 and 65 keV γ-lines assigned to the decay of ^{118}Ba. The solid lines show the best fits of the one-component decay curves to the experimental data.

Figure 9: Beta-strength distribution for the decay of $^{114-117}$Ba obtained in the pn-QRPA calculations [23] (solid histogram) and predicted by the gross theory [22] with "bottom raising" (dashed line).

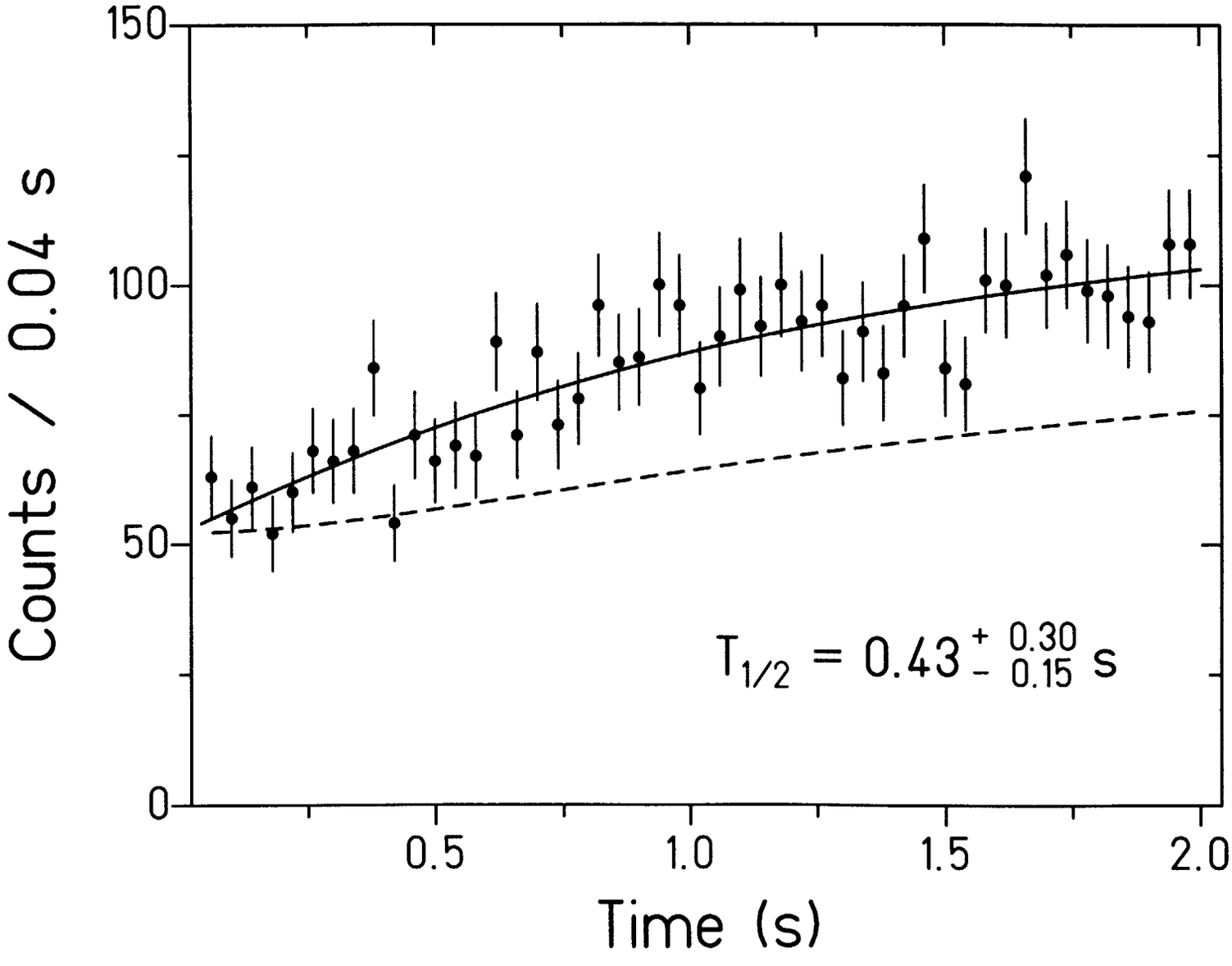

Fig. 1

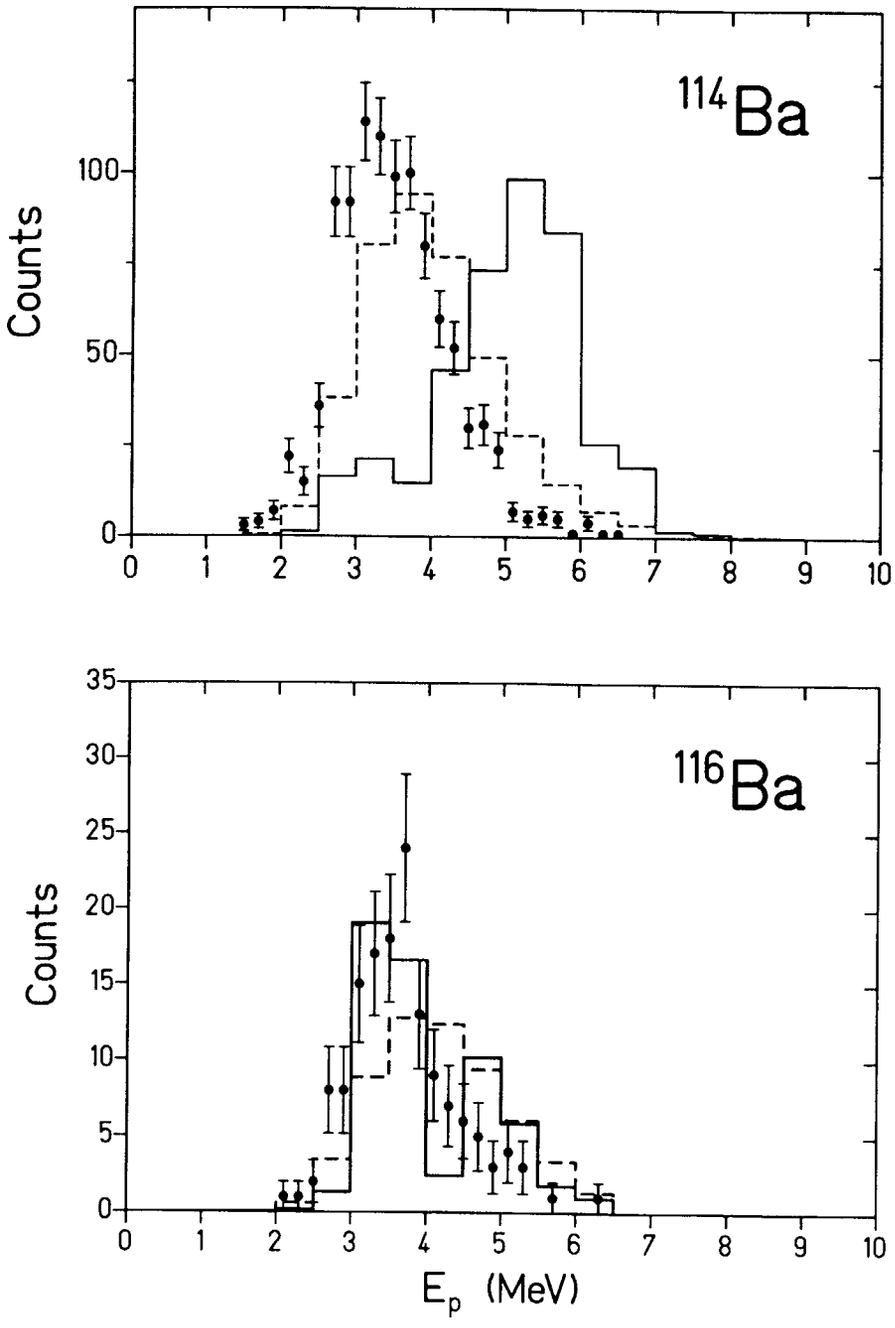

Fig. 2

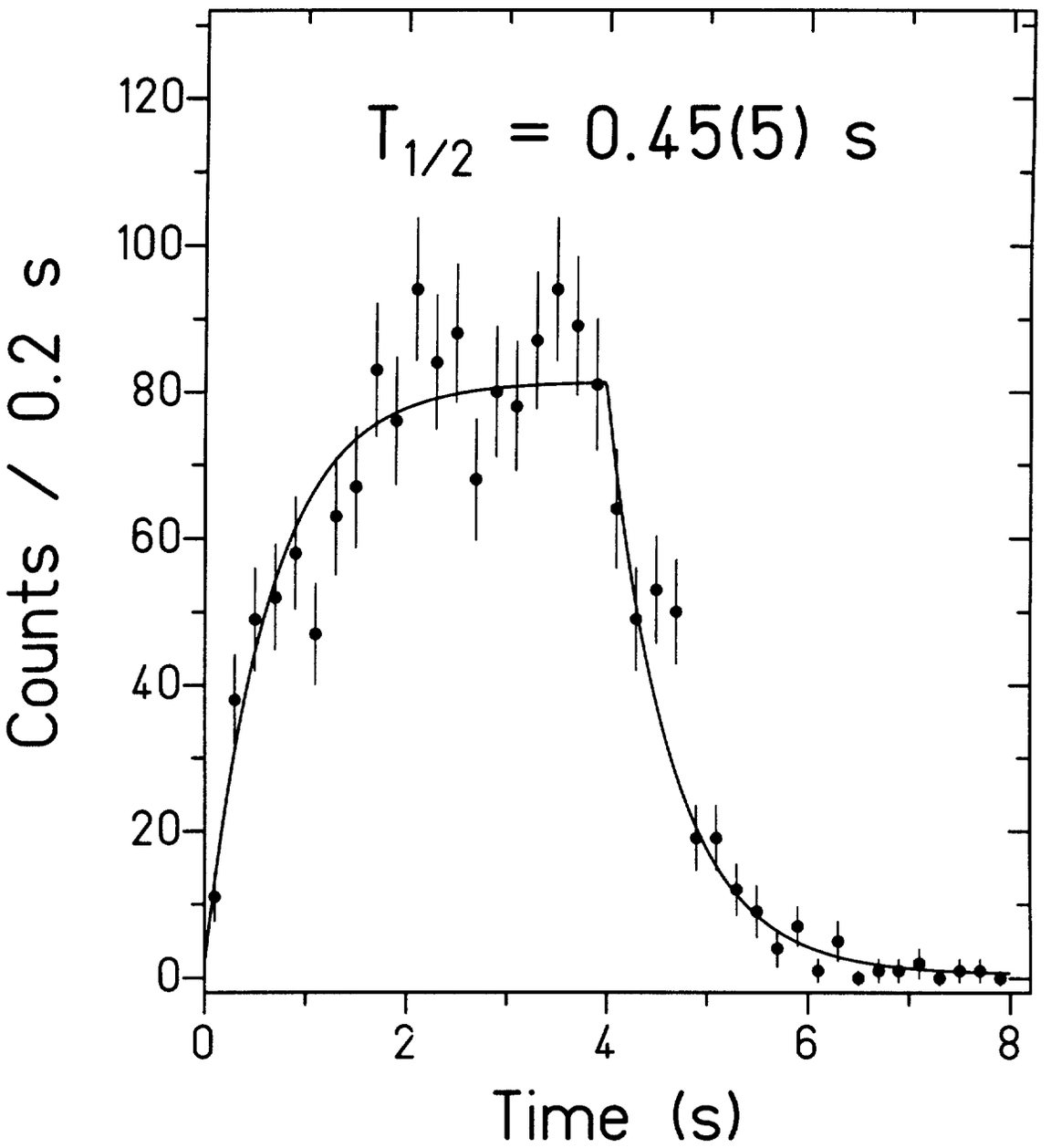

Fig. 3

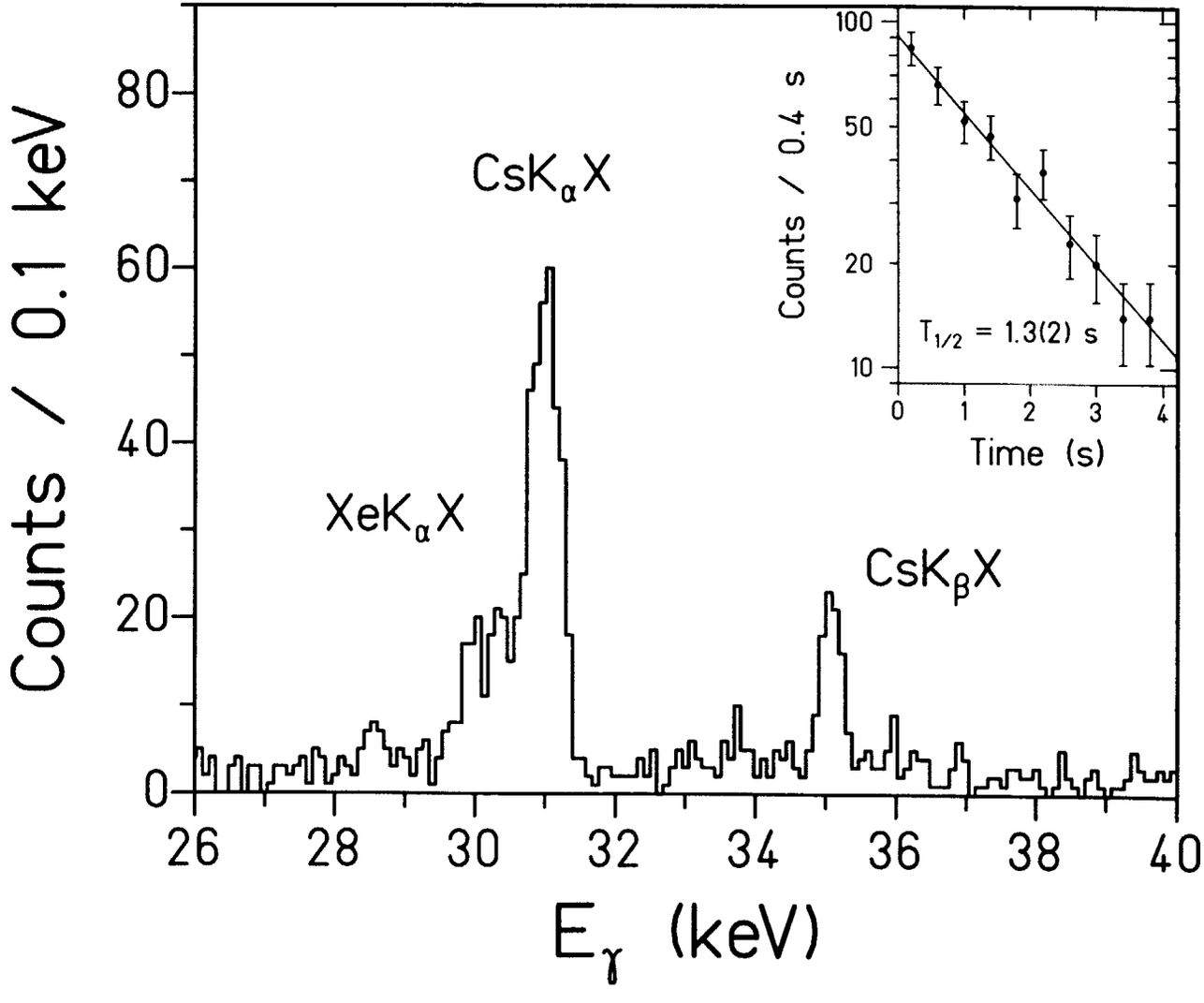
Counts / 0.1 keV
80
60
40
20
0
CsK$_\alpha$X
XeK$_\alpha$X
CsK$_\beta$X
26
28
30
32
34
36
38
40
E$_\gamma$ (keV)
Counts / 0.4 s
100
50
20
10
T$_{1/2}$ = 1.3(2) s
0
1
2
3
4
Time (s)

Fig. 4

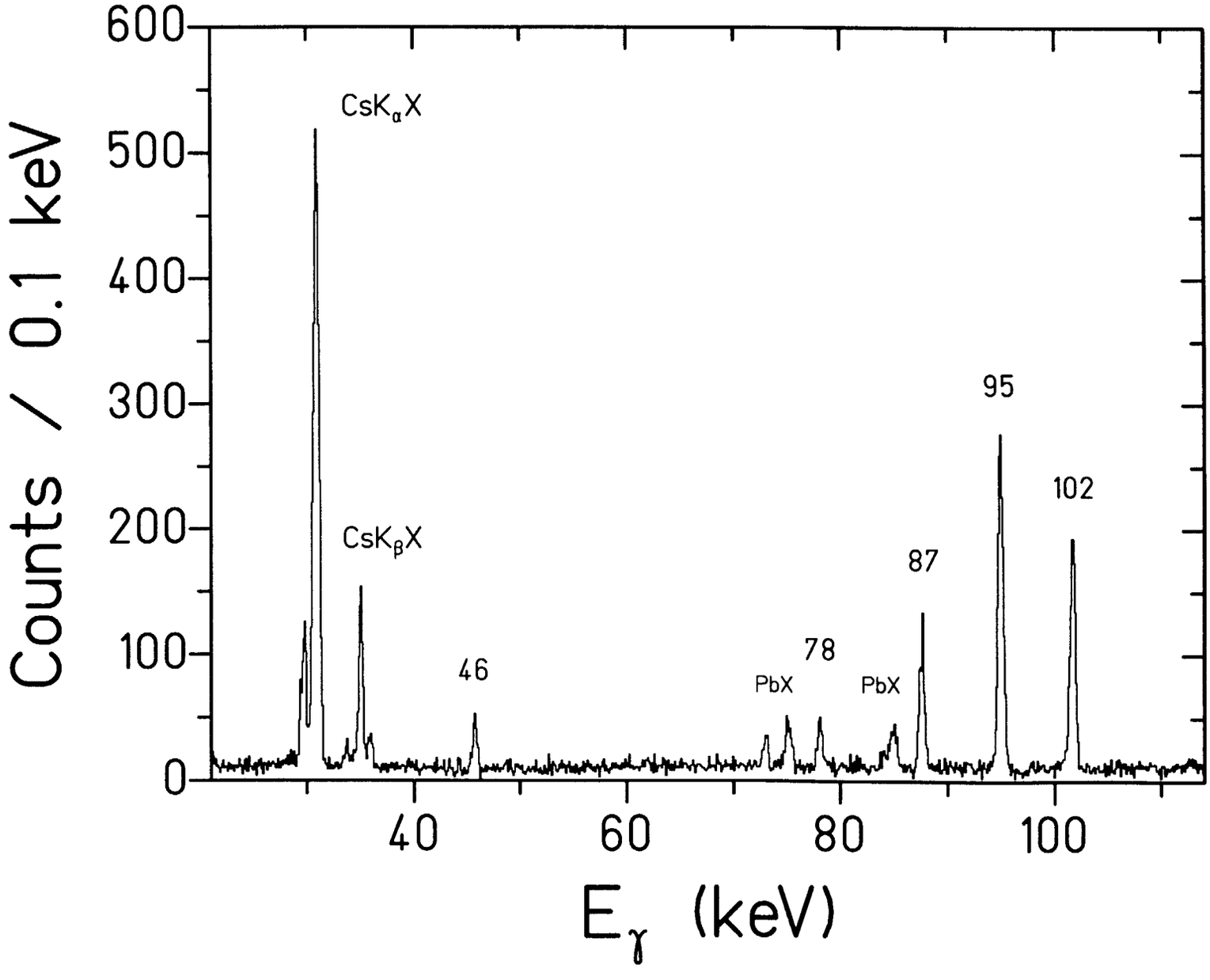
Counts / 0.1 keV
600
500
400
300
200
100
0
CsK$_\alpha$X
CsK$_\beta$X
46
PbX
78
PbX
87
95
102
40
60
80
100
E_γ (keV)

Fig. 5

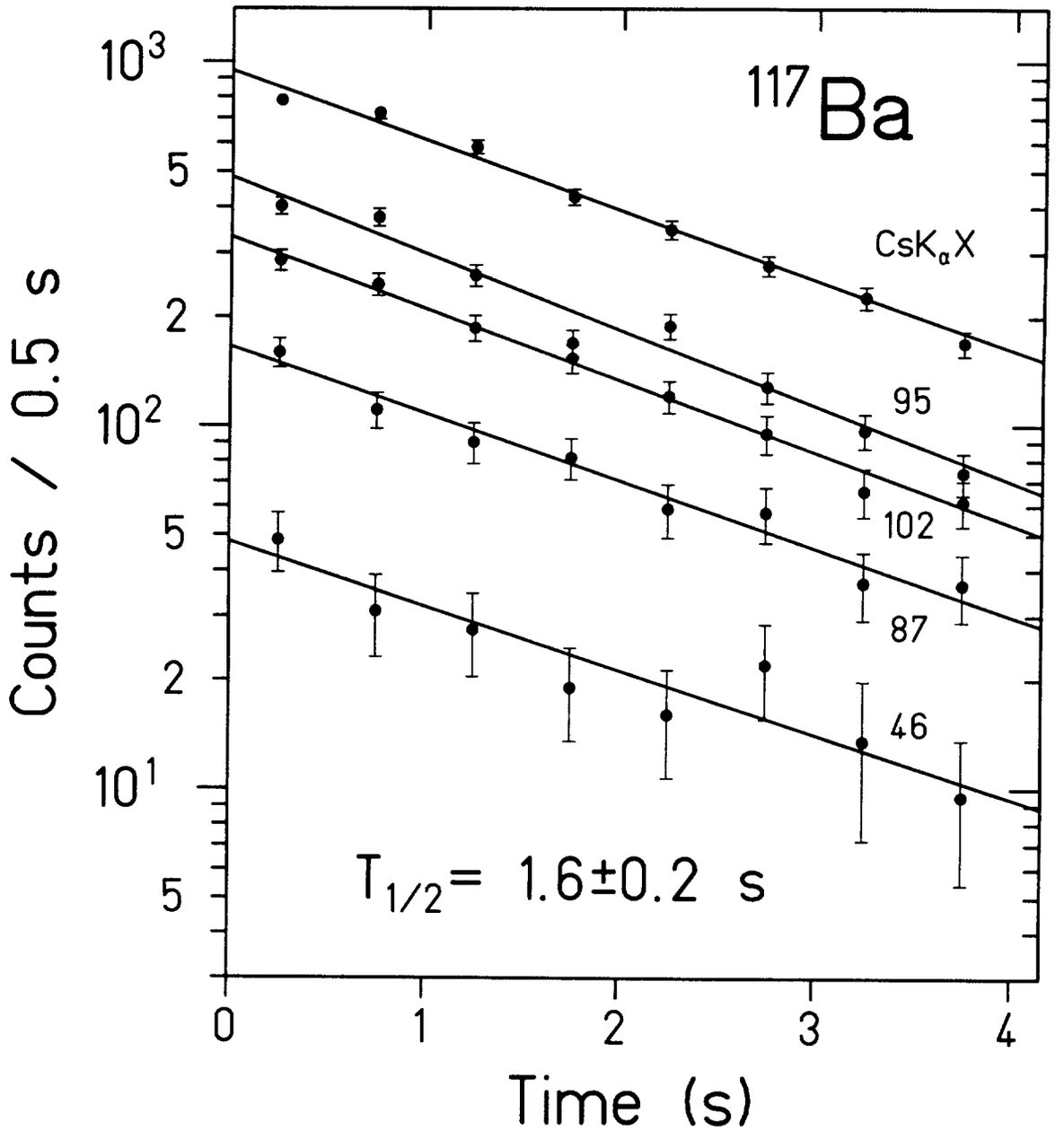
^{117}Ba
CsK$_\alpha$X
95
102
87
46
$T_{1/2}$= 1.6±0.2 s
Counts / 0.5 s
Time (s)
10^3
5
2
10^2
5
2
10^1
5
0
1
2
3
4

Fig. 6

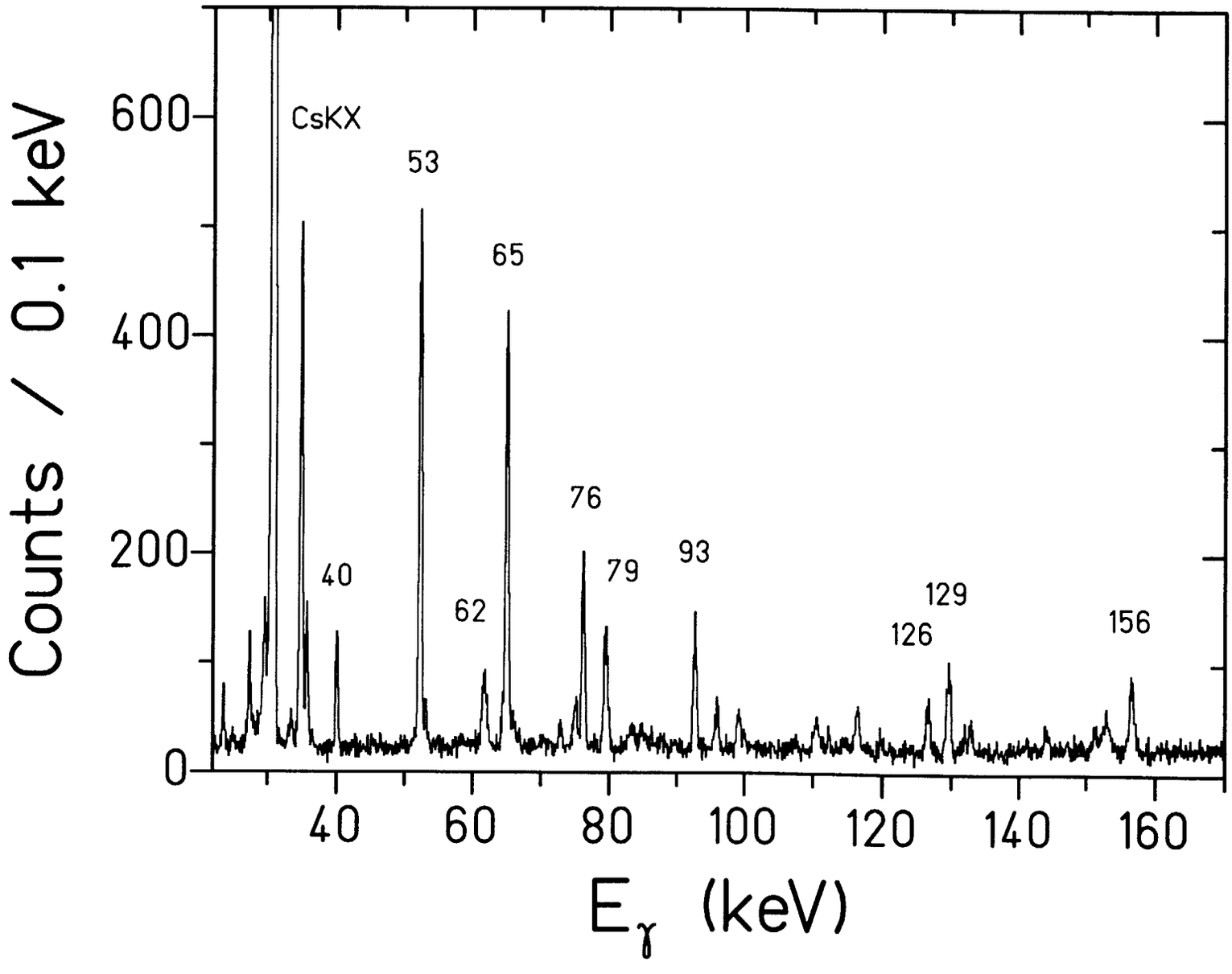
Counts / 0.1 keV
600
400
200
0
CsKX
53
65
76
40
62
79
93
129
126
156
40
60
80
100
120
140
160
E_γ (keV)

Fig. 7

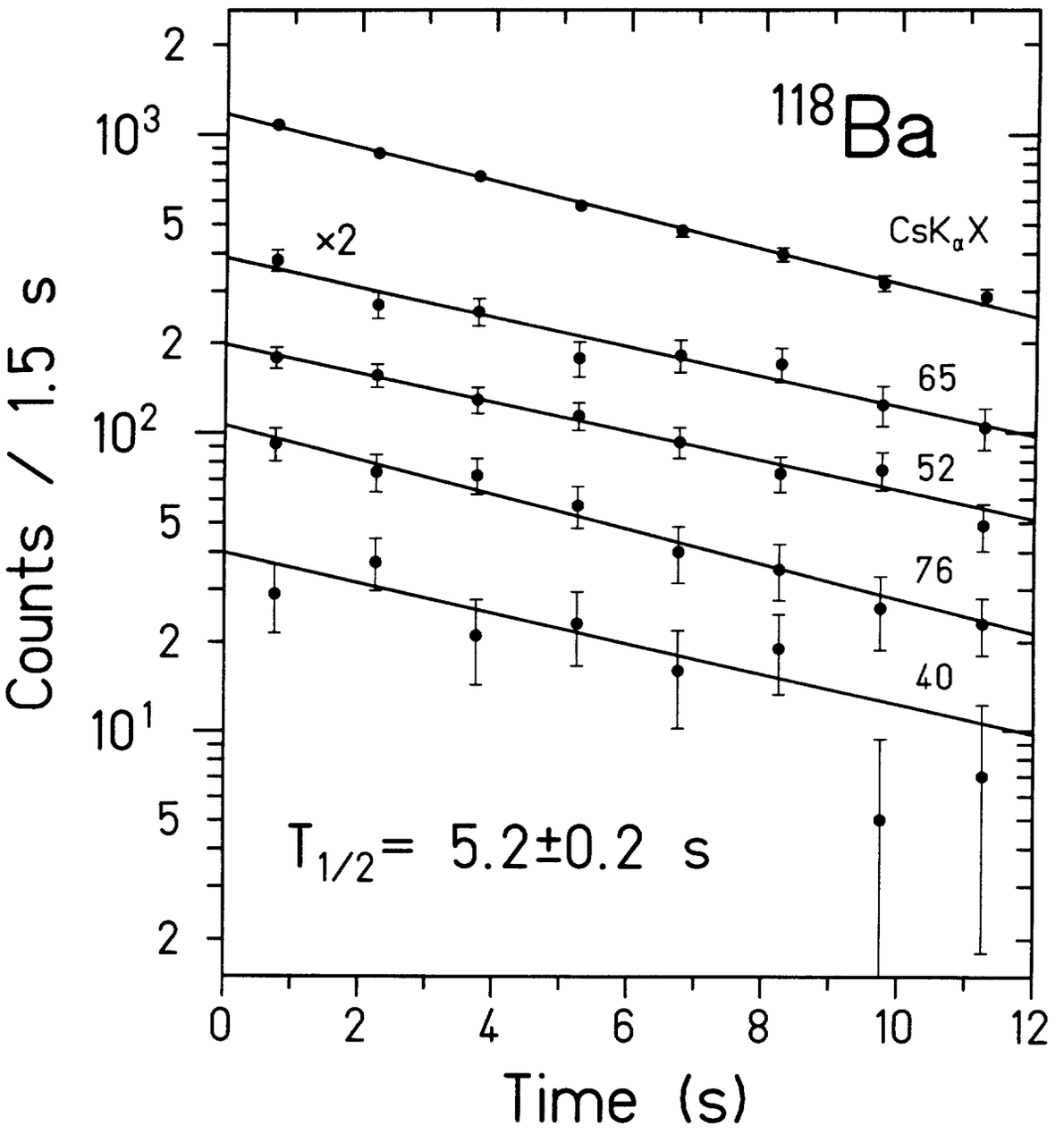
^{118}Ba
CsK$_\alpha$X
×2
65
52
76
40
$T_{1/2}$= 5.2±0.2 s
Counts / 1.5 s
Time (s)
2
10^3
5
2
10^2
5
2
10^1
5
2
0
2
4
6
8
10
12

Fig. 8

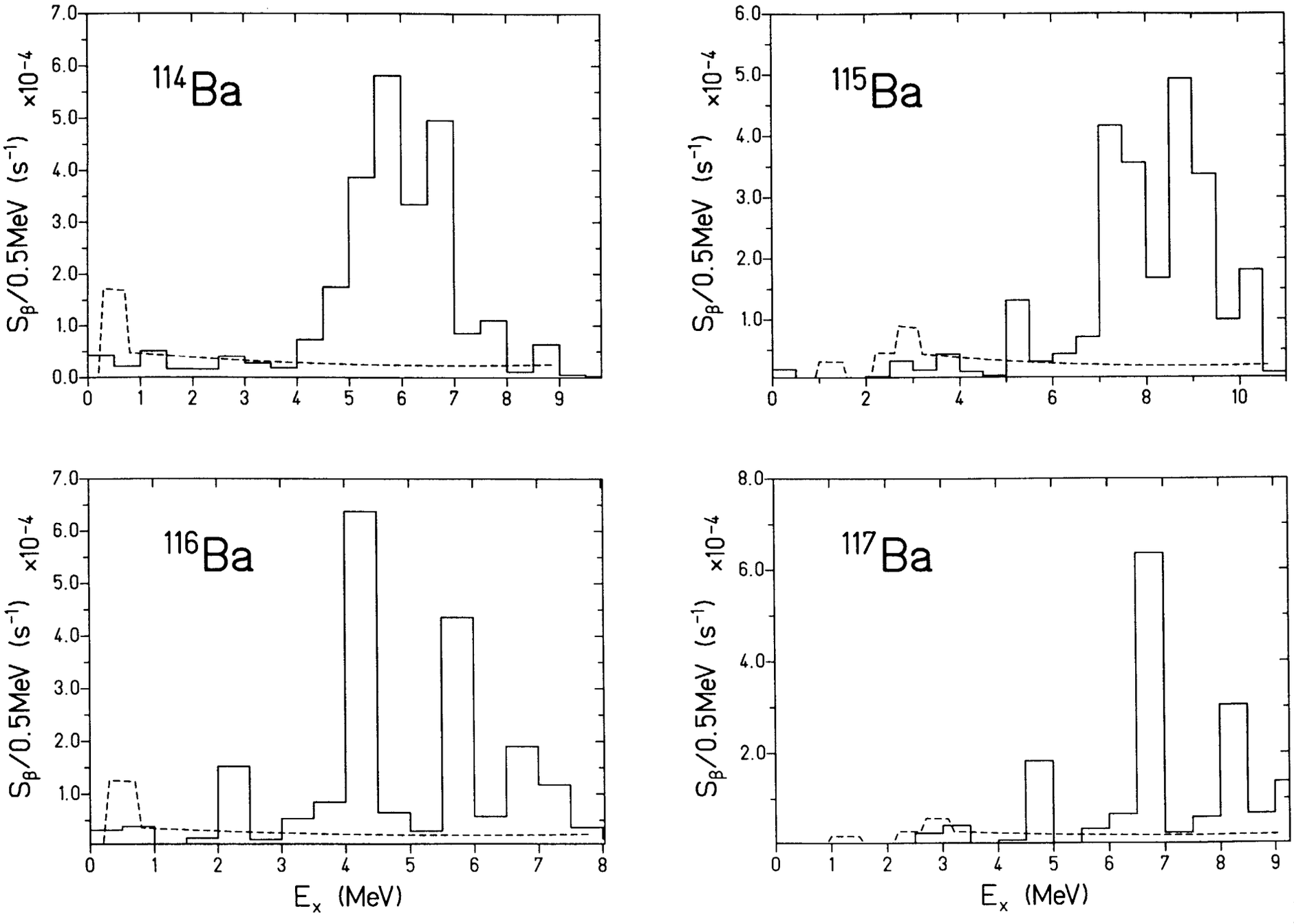

Fig. 9